EXAFS Data Indicate a "Normal" Axial Cobalt−Nitrogen Bond of the Organo-B_{12} Cofactor in the Two Coenzyme B_{12}-Dependent Enzymes Glutamate Mutase and 2-Methyleneglutarate Mutase

Frederic Champloy,[†] Gerwald Jogl,[†] Riikka Reitzer,[†] Wolfgang Buckel,[‡] Harald Bothe,[‡] Brigitta Beatrix,[‡] Gerd Broeker,[‡] Alain Michalowicz,[§] Wolfram Meyer-Klaucke,[||] and Christoph Kratky*,[†]

Contribution from the Abteilung für Strukturbiologie, Institut für Physikalische Chemie, Karl-Franzens-Universität, Heinrichstrasse 28, A-8010 Graz, Austria, Laboratorium für Mikrobiologie, Fachbereich Biologie, Phillipps-Universität, 35032 Marburg, Germany, GPMD Departement de Physique, URF Sciences, Université de Paris XII, Val de Marne, F-94010 Creteil, France, and European Molecular Biology Laboratory (EMBL), Outstation Hamburg, c/o DESY, Notkestrasse 85, D-22603 Hamburg, Germany

Received February 4, 1999. Revised Manuscript Received October 25, 1999

Abstract: A key step in the catalytic cycle of coenzyme B_{12}-dependent enzymes is the homolysis of the cofactor's organometallic bond, leading to the formation of a 5′-deoxyadenosyl radical. For the adenosylcobalamin-dependent enzyme methylmalonyl CoA mutase (MCM), it has been suggested that this step is mediated by a protein-induced lengthening of the cofactor's axial cobalt−nitrogen bond, in trans position to the scissile organometallic bond. In fact, such a lengthening was first observed in the crystal structure of MCM (Mancia et al. *Structure* **1996**, *4*, 339−350) and was later confirmed by an analysis of EXAFS data on the same protein in frozen solution (Scheuring et al. *J. Am. Chem. Soc.* **1997**, *119*, 12192−12200). Here, we report the results of an EXAFS study on the related coenzyme B_{12}-dependent enzymes glutamate mutase from *Clostridium cochlearium* and 2-methyleneglutarate mutase from *Clostridium barkeri*. Both apoenzymes were overproduced from *E. coli* and reconstituted with methylcobalamin (MeCbl) to yield inactive enzymes, whose stability toward (substrate-induced) cobalt−carbon bond homolysis should be higher than for the enzymatically active forms obtained by reconstitution with 5′-desoxyadenosylcobalamin. X-ray absorption data were collected around the cobalt K-absorption edge at 20 K on freeze-dried and frozen protein preparations. In addition to the two recombinant enzymes, we also collected XAS data on recombinant glutamate mutase, reconstituted with MeCbl in the presence of the inhibitor (2*S*,4*S*)-4-fluoroglutamate. As a reference compound for the interpretation of the EXAFS spectra, absorption data were also collected from crystalline MeCbl, whose crystal structure is known (Rossi et al. *J. Am. Chem. Soc.* **1985**, *107*, 1729−1738). The XANES parts of the XAS spectra for the four samples look very similar to one another and deviate significantly from the corresponding spectra of aquocob(III)alamin and for cob(II)alamin. Moreover, all four methyl-B_{12} spectra show a pronounced preedge peak, indicating the presence of a covalently attached sixth carbon ligand to the cobalt center. The EXAFS region of the protein spectra were simulated by deriving the amplitude reduction factor, the energy shift, and the Debye−Waller factors for each scattering path from the spectrum of the model compound. All geometrical parameters were assumed to be equal between model compound and enzyme-bound B_{12} cofactor, with the exception of the axial cobalt−nitrogen distance, which was varied between 1.7 and 2.9 Å. The resulting optimization profiles show the deepest minimums between 2.1 and 2.2 Å, close to the value observed for methylcobalamin. This is also true for the spectrum of GLM in the presence of inhibitor. In all simulations (including the one for the model compound), a second minimum appeared around 2.8 Å. In conclusion, our EXAFS evidence suggests a "normal" axial Co−N bond in the two coenzyme B_{12}-dependent enzymes glutamate mutase and 2-methyleneglutarate mutase. Although a very long (2.6−2.8 Å) Co−N bond would also be compatible with the observed spectra, it is considered unlikely.

Introduction

Homolysis of the B_{12} cofactor's cobalt−carbon bond leading to the formation of a 5′-deoxyadenosyl radical[1] is one of the key steps in the catalytic cycle of coenzyme B_{12}-dependent enzymes, such as methylmalonyl CoA mutase (MCM), glutamate mutase (GLM), or 2-methyleneglutarate mutase (MGM). The way the apoenzyme mediates and assists this process has been a long-standing question in B_{12} research.

The rate of enzymatically accelerated substrate-induced homolytic cobalt−carbon bond cleavage of coenzyme B_{12} (AdoCbl; see Figure 1) exceeds the rate observed in aqueous solution of AdoCbl by about 12 orders of magnitude,[1,2] as a

* Corresponding author: tel, +43 316 380 5417; fax, +43 316 380 9850; e-mail, Christoph.Kratky@kfunigraz.ac.at.
[†] Universität Graz.
[‡] Universität Marburg.
[§] Université de Paris XII.
[||] EMBL Outstation Hamburg.
(1) Halpern, J. *Science* **1985**, *227*, 869−75.

10.1021/ja990349q CCC: $18.00
Published on Web 12/02/1999

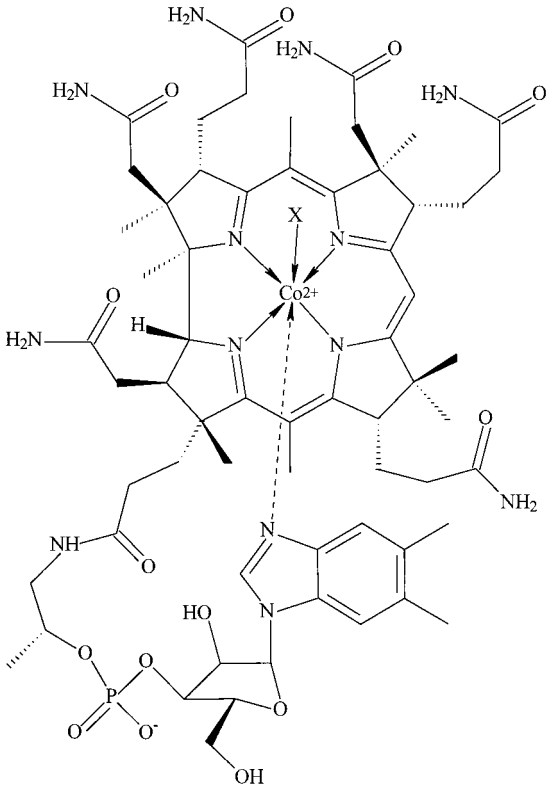

Figure 1. Structural formulas of B_{12} compounds: 5′-desoxyadenosylcobalamin (AdoCbl, X = 5′-desoxyadenosyl$^-$); methylcobalamin (MeCbl, X = CH_3^-); aquocobalamin (AqCbl, X = H_2O); Cob(II)alamin (B_{12r}, X = e^-). Note that the terms $AqoB_{12}$, $AdoB_{12}$, and MeB_{12} are used for the corresponding cobalamin species after binding to protein, with possible replacement of the intramolecular coordination of the dimethylbenzimidazole base by a protein-derived imidazole.

result of the interaction of $AdoB_{12}$ with the apoenzyme in the presence of substrate. One hypothesis to account for this rate enhancement invoked a protein-mediated distortion of the B_{12} molecule ("mechanochemical distortion"),[3] originally proposed to consist of a flexing of the corrinoid macrocycle resulting in a weakening of the Co−C bond.[3−6] This mechanochemical hypothesis was challenged several years ago by the result of the crystal structure analysis of the corrinoid homolysis product cob(II)alamin, which showed a molecular conformation very similar to that of the intact AdoCbl.[7] If a protein-mediated deformation of the B_{12} moiety should be catalytically effective, it is necessary that the deformed geometry is "more similar" to the Co(II) reaction product than the undeformed adenosyl-B_{12} species. Therefore, apoenzyme/coenzyme interactions at the corrin moiety were considered insufficient to provide the major means for protein-induced activation of bound coenzyme B_{12} toward homolysis. Instead, it was suggested "that the organometallic bond may be labilized largely by way of apoenzyme (and substrate) induced separation of the homolysis fragments, made possible by strong binding of both separated fragments to the protein". Recent crystallographic results on the coenzyme B_{12}-dependent enzyme methylmalonyl CoA mutase showed large differences in conformation between substrate-free and substrate-bound enzyme,[8,9] strongly suggesting that such a mechanism is indeed significant in MCM.

Most known 3D structures of B_{12}-dependent enzymes or enzyme fragments[10−12] show the intramolecular cobalt coordination of the dimethylbenzimidazole base (DMB) to be replaced by the metal coordination of a protein-derived imidazole. Notably, the bond between cobalt and the coordinating ϵ-nitrogen (Nϵ2) of His-A610 was observed unexpectedly long in the MCM crystal structure:[11] values for the axial Co−N bond between 1.93[13] and 2.21[14] Å have been observed for the axial Co−N bond length in crystal structures of various cobalamins, in contrast to 2.53 Å reported for the MCM structure.[11] This elongated bond was proposed to put the cobalt into a strained state, favoring the formation of the adenosyl radical,[11] thus reviving the mechanochemical distortion theory. In fact, a structural correlation[15] was suggested to support a mechanism involving labilization of the Co−C bond by stretching the transannular Co−N bond.

The crystal structure analysis of MCM was complicated by disorder of the B_{12} cofactor, which occurred as a mixture of Co(II) and Co(III) species, with the former predominating. However, a long axial Co−N bond for MCM with AdoCbl was also observed by EXAFS.[16] Recent crystallographic data on substrate-free MCM[8] again indicated a long axial Co−N bond, but suggested another mechanism for the enzyme-mediated adenosyl radical formation: upon binding of substrate, a conformational change occurs in the protein that drives the adenosyl group off the cobalt atom. The long $Co-N_{ax}$ bond was suggested to contribute to the weakening of the cobalt−carbon bond, but might also be a way for the apoenzyme to discriminate between adenosylcobalamin (which it tightly binds) and hydroxocobalamin (which is less tightly bound).

Very recently, refinement of the crystal structure of glutamate mutase from *Clostridium cochlearium*,[17] reconstituted with methylcobalamin (MeCbl) and CNCbl, was concluded in our laboratory.[12] As in MCM, an elongation of the axial Co−N bond was observed for both cofactors by about 0.3 Å, as compared to what one might expect from structures of isolated cofactors. However, as in MCM, the cofactor occurred as a mixture of several species containing different cobalt oxidation states. While the two GLM structures thus corroborate the previous observation of an elongated axial Co−N bond, neither the origin for the bond elongation nor the exact chemical nature of the cofactor with a long bond emerged from these structures.

Recently, the crystal structure analysis of diol dehydratase was published, the first case of a coenzyme B_{12}-dependent enzyme with the cofactor in "base-on" constitution.[18] While a

(2) Hay, B. P.; Finke, R. G. *J. Am. Chem. Soc.* **1986**, *108*, 4820−4829.
(3) Schrauzer, G. N.; Grate, J. H.; Hashimoto, M.; Maihub, A. In *Vitamin B_{12}*; Zagalak, B., Friedrich, W., Eds.; W. deGruyter: Berlin, 1979; pp 511−528.
(4) Bresciani-Pahor, N.; Forcolin, M.; Toscano, P. J.; Summers, M. F.; Randaccio, L.; Marzilli, L. G. *Coord. Chem. Rev.* **1985**, *63*, 1−125.
(5) Chemaly, S. M.; Pratt, J. M. *J. Chem. Soc., Dalton Trans.* **1980**, 2274−2281.
(6) Hay, B. P.; Finke, R. G. *J. Am. Chem. Soc.* **1987**, *109*, 8012−8018.
(7) Kräutler, B.; Kratky, C.; Keller, W. *J. Am. Chem. Soc.* **1989**, *111*, 8936−8938.
(8) Mancia, F.; Evans, P. R. *Structure* **1998**, *6*, 711−720.
(9) Mancia, F.; Smith, G. A.; Evans, P. R. *Biochemistry* **1999**, *38*, 7999−8005.
(10) Drennan, C. L.; Huang, S.; Drummond, J. T.; Matthews, R. G.; Ludwig, M. L. *Science* **1994**, *266*, 1669−1674.
(11) Mancia, F.; Keep, N. H.; Nakagawa, A.; Leadlay, P. F.; McSweeney, S.; Rasmussen, B.; Bosecke, P.; Diat, O.; Evans, P. R. *Structure* **1996**, *4*, 339−350.
(12) Reitzer, R.; Gruber, K.; Jogl, G.; Wagner, U. G.; Bothe, H.; Buckel, W.; Kratky, C. *Structure* **1999**, *7*, 891−902.
(13) Kratky, C.; Färber, G.; Gruber, K.; Wilson, K.; Dauter, Z.; Nolting, H.-F.; Konrat, R.; Kräutler, B. *J. Am. Chem. Soc.* **1995**, *117*, 4654−4670.
(14) Lenhert, P. G. *Proc. R. Soc. (London)* **1968**, *A303*, 45−84.
(15) De Ridder, D. J. A.; Zangrando, E.; Bürgi, H.-B. *J. Mol. Struct.* **1996**, *374*, 63−83.
(16) Scheuring, E.; Padmakumar, R.; Banerjee, R.; Chance, M. R. *J. Am. Chem. Soc.* **1997**, *119*, 12192−12200.
(17) Reitzer, R.; Krasser, M.; Jogl, G.; Buckel, W.; Bothe, H.; Kratky, C. *Acta Crystallogr.* **1998**, *D54*, 1039−1042.

long axial Co−N bond (~2.5 Å) was again observed, the electron density of the "upper" ligand was diffuse, possibly as a result of X-ray-induced bond cleavage. Thus, as in the other enzymes, the oxidation state of the cobalt center is unclear.

Whatever is the functional significance of the long axial Co−N bond, its observation in several different coenzyme B_{12}-dependent enzymes is intriguing. There is a general belief that all coenzyme-B_{12}-dependent mutases operate via a radical mechanism[19−21] initiated by homolysis of the cofactor's cobalt−carbon bond. While there can be little doubt about the relevance of the mechanism for enzyme-induced homolysis suggested on the basis of the structure of substrate-free MCM,[8] the question remains whether a long axial Co−N bond of the cofactor is also a functional component for this event. At present it is also unclear which of the B_{12} species present in the crystals of GLM and MCM show the elongated bond.

Here, we report the results of a determination of the axial Co−N bond length in the two adenosylcobalamin-dependent enzymes glutamate mutase and 2-methyleneglutarate mutase by EXAFS spectroscopy. Biological EXAFS spectroscopy is an ideal complement to X-ray crystallography to answer specific questions relating to the coordination around metal atoms.[22] While it does not depend on the availability of crystalline material, it can yield metal−ligand distances with an accuracy approaching 0.01 Å under favorable circumstances. However, the method has its pitfalls in the form of false minimums, and it requires the availability of a model complex with precisely known 3D structure.

GLM from *C. cochlearium*, which equilibrates (*S*)-glutamate with (2*S*,3*S*)-3-methylaspartate,[23,24] has been characterized as a stable heterotetramer ($\epsilon_2\sigma_2$) containing two molecules of coenzyme B_{12}.[12] While the cofactor of the enzyme from the related organism *Clostridium tetanomorphum* has been identified as pseudocoenzyme B_{12}, in which the axial base dimethylbenzimidazole has been replaced by adenine,[25,26] a mixture of pseudovitamin B_{12} and factor A (2-methyladeninlylcyanocobamide) has been isolated from a cyanolysate of *C. cochlearium*. However, the enzyme also shows high activity with coenzyme B_{12} as cofactor. This is not surprising, since in the active complex the conserved histidine residue 16 of the σ polypeptide, rather than dimethylbenzimidazole, is coordinated to the cobalt.[12,27] The genes *glmE* and *glmS* coding for the polypeptides ϵ and σ, respectively, have been cloned and overexpressed separately in *Escherichia coli*. Upon purification, polypeptide σ (m = 14.7 kDa), which has been designed as component S, is obtained as a monomer, whereas the other polypeptide forms a dimer (ϵ_2, m = 107 kDa) and was called component E.[27−29]

MGM is involved in the rearrangement of 2-methyleneglutarate to (*R*)-3-methylitaconate.[30] The enzyme from *Clostridium barkeri* was shown to be a homotetramer (α_4, 269 kDa).[31] Its gene was cloned, sequenced, and overexpressed in *E. coli*.[32] Active 2-methyleneglutarate mutase containing two adenosylcobalamin molecules is obtained in a manner similar to glutamate mutase by reconstituting the recombinant gene product with coenzyme B_{12}.

When the EXAFS experiments were designed, it was decided to investigate the two enzymes reconstituted with MeCbl instead of the active cofactor 5′-desoxyadenosylcobalamin. When bound to the apoenzyme, the latter cofactor becomes unstable and prone to homolysis of its cobalt−carbon bond, which may then lead to a mixture of enzymes containing different cofactors (such as aquo-B_{12} or Co^{II}-B_{12}). Such problems have hampered the MCM crystal structure analysis.[11]

Materials and Methods

Sample Preparation. *Methylcobalamin* for the EXAFS experiment was purchased from Sigma and validated by UV/visible spectroscopy. Sample preparation aimed at a difference $\Delta\mu x$ in the absorption coefficient before and after the absorption edge (edge jump) between 1 and 2: 100 mg of crystals was crushed and a pellet of 1 mm thickness was formed from pure solid MeCbl without any powdered diluent. This pellet was sealed in a 1 cm^2 sample holder between two layers of Mylar tape. All operations involving MeCbl were carried out under red light conditions in order to prevent photolysis. The integrity of the sample was controlled by UV/visible spectroscopy of dissolved MeCbl before and after exposure to X-rays, yielding no detectable change.

Recombinant glutamate mutase from *C. cochlearium* was prepared as the isolated apoenzyme components as described previously:[17] *E. coli* strain MC 4100 containing the expression vector pOZ3[29] and *E. coli* strain DH5α containing pOZ5[28] were used for overproduction of glutamate mutase components S and E, respectively. The bacteria were grown to $OD_{600} \approx 1$ on standard 1 nutrient broth (Merck, Darmstadt, Germany), induced overnight with 1 mM isopropyl-1-thio-β-D-galactoside (IPTG), and harvested by centrifugation. Enzyme activity was measured on samples reconstituted with AdoCbl using the spectrophotometric assay developed by Barker et al.[23] For the purification, the procedure described in ref 33 was used.

For the recombination with MeCbl to yield the inactive glutamate mutase, component E was incubated at +37 °C for 10 min with a 3 times molar excess of component S and 6 times molar excess of MeCbl under red light conditions. The excess of component S was essential in order to avoid the contamination of the recombinant inactive enzyme by homodimer component E. After incubation, the sample was applied to a size exclusion chromatography column (Superdex 200, Pharmacia) and the purity of the red glutamate mutase-containing fractions was monitored by PAGE in the absence and presence of SDS.

The inhibitor (2*S*,4*S*)-4-fluoroglutamate was purchased from V. Tolman (P.O. Box 143 00, Praha 412, Czech Republic). A 10-fold molar excess of the inhibitor was added to the GLM−MeCbl preparation for the experiments with added inhibitor.

(a) Isothermal Titrating Calorimetry. To ensure that (2*S*,4*S*)-4-fluoroglutamate—which is a strong inhibitor for the intact glutamate mutase[34]—also binds to inactive glutamate mutase reconstituted with MeCbl, we performed an isothermal titration calorimetry experiment, in which a solution of the protein was titrated with the inhibitor. Experiments were carried out with a MicroCal MCS-ITC instrument.

(18) Shibata, N.; Masuda, J.; Tobimatsu, T.; Toraya, T.; Suto, K.; Morimoto, Y.; Yasuoka, N. *Structure* **1999**, *7*, 997−1008.
(19) Buckel, W.; Golding, B. T. *Chem. Soc. Rev.* **1996**, *25*, 329−337.
(20) Golding, B. T.; Buckel, W. In *Comprehensive Biological Catalysis*; Sinnott, M., Ed.; Academic Press: London, 1998; Vol. 3, pp 239−259.
(21) Rétey, J. *Angew. Chem.* **1990**, *102*, 373−379.
(22) Bertagnolli, H.; Ertel, T. S. *Angew. Chem.* **1994**, *106*, 15−37.
(23) Barker, H. A.; Rooze, V.; Suzuki, F.; Iodice, A. A. *J. Biol. Chem.* **1964**, *239*, 3260−3266.
(24) Switzer, R. L. In *Glutamate mutase*; Dolphin, D., Ed.; Wiley-Interscience: New York, 1982; Vol. 2, pp 289−355.
(25) Barker, H. A.; Weissbach, H.; Smyth, R. D. *Proc. Natl. Acad. Sci. U.S.A.* **1958**, *44*, 1993−1997.
(26) Friedrich, W. *Vitamin B_{12} und verwandte Corrinoide*; Thieme Verlag: Stuttgart, 1975; Vol. III/2.
(27) Zelder, O.; Beatrix, B.; Kroll, F.; Buckel, W. *FEBS Lett.* **1995**, *369*, 252−254.
(28) Zelder, O.; Beatrix, B.; Leutbecher, U.; Buckel, W. *Eur. J. Biochem.* **1994**, *226*, 577−585.
(29) Zelder, O.; Beatrix, B.; Buckel, W. *FEMS Microbiol. Lett.* **1994**, *118*, 15−22.
(30) Kung, H.-F.; Cederbaum, S.; Tsai, L.; Stadtman, T. C. *Proc. Natl. Acad. Sci. U.S.A.* **1970**, *65*, 978−984.
(31) Michel, C.; Hartrampf, G.; Buckel, W. *Eur. J. Biochem.* **1989**, *184*, 103−107.
(32) Beatrix, B.; Zelder, O.; Linder, D.; Buckel, W. *Eur. J. Biochem.* **1994**, *221*, 101−109.
(33) Bothe, H.; Darley, D. J.; Albracht, S. P. J.; Gerfen, G. J.; Golding, B. T.; Buckel, W. *Biochemistry* **1998**, *37*, 4105−4113.
(34) Leutbecher, U.; Bocher, R.; Linder, D.; Buckel, W. *Eur. J. Biochem.* **1992**, *205*, 759−765.

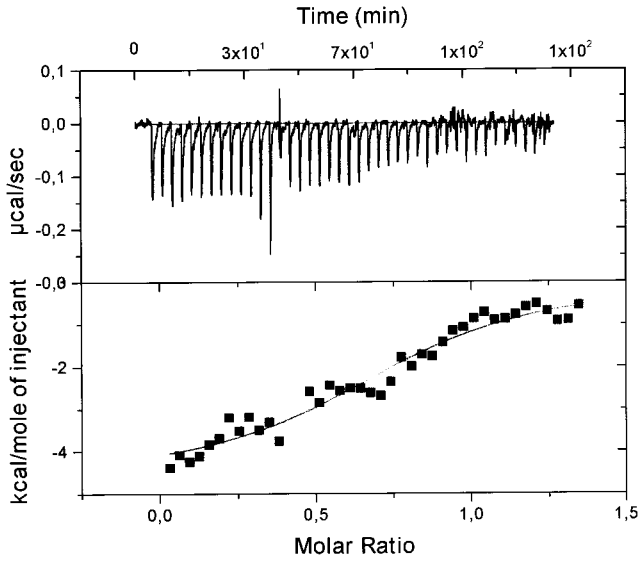

Figure 2. (a, top) Experimental trace (heat per second versus time) for the isothermal titration of glutamate mutase with the inhibitor (2*S*,4*S*)-4-fluoroglutamate. The negative peaks show that the inhibitor binding is exothermic. (b, bottom) integrated heats (kilocalorie per mole of inhibitor injected) for each injection plotted versus the molar ratio of inhibitor to glutamate mutase.

After protein purification following the reconstitution with MeCbl, the enzyme concentration was checked by UV/visible spectroscopy at 280, 339, 375, and 527 nm. The cell was filled with 1.36 mL of a solution with a protein concentration of 35 μM in 50 mM phosphate buffer pH 7.4. The inhibitor at a concentration of 0.5 mM in water was added in 41 injections of 2.997 μL, each with a dead time of 3 min and a preincubation time of 10 min at 30 °C. The experimental trace as well as a plot of integrated heat versus injection volume are shown in Figure 2. From these data, a molecular ratio of 0.7($\pm$0.03) molecules of inhibitor per B_{12} molecule, a dissociation constant K of 3.9($\pm$0.8) μM, and a reaction enthalpy ΔH_0 of $-4.6(\pm 0.2)$ kcal/mol could be computed, using version 2.9 of the program package ORIGIN. The previously observed kinetic inhibition constant K_i from the enzyme reconstituted with adenosylcobalamin is 70 μM.[34]

(b) Preparation and Purification of Recombinant 2-Methyleneglutarate Mutase from *C. barkeri.* The protein was overproduced in *E. coli* strain DH5a containing the expression vector pBB2.[32] Bacteria were grown to $OD_{574} = 1$ on standard 1 nutrient broth (Merck), induced with 200 μM IPTG, and harvested by centrifugation.

Enzyme activity was assayed using a spectrophotometric assay.[31] Purification procedures were monitored by SDS−PAGE. For purification of recombinant 2-methyleneglutarate mutase, harvested *E. coli* cells were resuspended in buffer A (50 mM potassium phosphate pH 7.4, 1 mM EDTA, 2 mM DTT) and sonicated three times for 2 min followed by centrifugation. The supernatant was applied to a Q-Sepharose column (Hiload 26/10, Pharmacia) previously equilibrated with buffer A. An increasing linear gradient was applied to 1 M NaCl (800 mL, buffer A to buffer B: 50 mM potassium phosphate pH 7.4, 1 mM EDTA, 2 mM DTT, 1 M NaCl).

Fractions containing active 2-methyleneglutarate mutase were pooled, and solid ammonium sulfate was added to a final concentration of 1 M. The solution was applied to a phenyl-Sepharose column (HiLoad 26/10, Pharmacia) previously equilibrated with buffer C (50 mM potassium phosphate pH 7.4, 1 mM EDTA, 2 mM DTT, 1 M ammonium sulfate). A decreasing linear gradient (buffer C to buffer A, 200 mL) was applied. Fractions containing 2-methyleneglutarate mutase were concentrated to less than 5 mL using Millipore Ultrafree-15 filter units with Biomax-10K membranes (Sigma). The concentrate was applied to a Superdex 200 column and eluted with buffer A.

For the reconstitution with MeCbl, the purified protein was incubated with an at least 2-fold molar excess of MeCbl and run through the size-exclusion column (Superdex 200, buffer A) to remove the excess of B_{12}.

(c) Preparation of Protein Samples for EXAFS Data Collection. All protein preparations were freeze-dried, and the powder was mixed with glycerol. The slurries were packed into 1 mm sample holders between two Kapton foils and immediately dumped into liquid nitrogen. Each sample contained about 75 mg of protein. All preparation steps following the addition of MeCbl were carried out under red light. Following the EXAFS experiments, sample integrity was checked by UV/visible spectroscopy (see Figure 10) and SDS−PAGE from redissolved material.

Collection of XAS Data. (a) Methylcobalamin. The XAS data were collected in absorption mode at LURE-DCI EXAFS III station in Orsay, France. The major components of the beam line include a bending magnet and a double crystal Si(311) monochromator with a fixed exit. For harmonic rejection, the monochromator is detuned to 20%. The energy resolution of the spectrometer is 2.0 eV, and it was calibrated with a Co metal foil. During the experiments, the samples were located in the He exchange gas atmosphere (20 K) of a closed-cycle cryostat. I and I_0 were measured in the range of 7400−8650 eV using two low-pressure air-filled ionization chambers. The gas pressure was adjusted to obtain less than 2 mA current. All measurements were carried out with the DCJ ring operating with a positron bunch at an energy of 1.85 GeV and a current of 250 mA (250 h lifetime).

Energy scans were repeated several times and merged. The value observed for $\Delta\mu x$ was 1.25. The spectrum was calibrated according to the data observed for the Co metal foil. The merging and deglitching of the data were performed with the program suite "EXAFS pour le Mac".[35]

(b) Glutamate Mutase and 2-Methyleneglutarate Mutase. The XAS data were collected in fluorescence mode at the EMBL-EXAFS station (D2) at DESY in Hamburg, Germany. The major components of the beam line include a bending magnet, a double-crystal Si(111) monochromator, a focusing Au coated mirror with a cutoff energy of 21 keV, and an energy calibration device.[36−38] For harmonic rejection, the monochromator was detuned to 50% of its peak intensity. The energy resolution of the spectrometer was 2.0 eV as established from the full width at half-maximum of the calibrator Bragg peaks. During the experiments, the samples were located in the He exchange gas atmosphere (20 K) of a closed-cycle cryostat. I_f was measured in the range from 7500 to 8700 eV using a Camberra 13 element detector (energy resolution 300 eV) under 90° to the incoming beam, I_o was measured with a He ion chamber in front of the sample holder. All measurements were carried out at the DORIS III ring operating with a positron bunch at an energy of 4.48 GeV and a current of 120−60 mA.

Scans were repeated several times for each sample (50−100); every scan was individually energy calibrated according to the Bragg peak of the calibration device chosen at 7900 eV ([6 2 0] reflection of the calibrator). Each scan was checked for the presence of the preedge peak characteristic of a sixth covalently attached ligand (a methyl in our case), indicating that the sample was stable during the measurement. All the spectra were then averaged with the computer programs developed at the EMBL outstation.[39] Sharp glitches were removed manually, using a third-order polynomial.

The observed $\Delta\mu x$ values were 0.13 for MGM, 0.06 for GLM without inhibitor, and 0.025 for GLM with inhibitor.

Analysis of XAS Data. (a) Data Reduction and Normalization. The data reduction was performed using the computer program WinXas 2.4[40] on a Pentium PC. All spectra were normalized using the same protocol. E_0 was determined as 7735($\pm$2) eV, from the inflection point of the edge jump, i.e., by determining the maximum in the first derivative of the spectrum. The normalization was performed with the

(35) Michalowicz, A. *EXAFS pour le Mac*; Société Française de Chimie: Paris, 1991; pp 102−103.
(36) Hermes, C.; Gilberg, E.; Koch, M. H. *Nucl. Instrum. Methods* **1984**, *222*, 207−214.
(37) Petiffer, R. F.; Hermes, C. *J. Appl. Crystallogr.* **1985**, *18*, 404−412.
(38) Petiffer, R. F.; Hermes, C. *J. Phys. (Paris)* **1986**, *47*, 127−133.
(39) Nolting, H. F.; Hermes, C. C. In *EXPROG: EMBL-EXAFS data analysis and evaluation program for PC/AT*; Nolting, H. F., Hermes, C., Ed.; European Molecular Biology Laboratory: Hamburg, 1992.
(40) Ressler, T. *J. Synchrotron Rad.* **1998**, *5*, 118−122.

Lengeler−Eisenberger procedure:[41,42] the preedge region was fitted with a first-order polynomial, the $k^3\chi(k)$ signal of the postedge region with a fifth-order polynomial followed by a six-knot spline fit. The obtained EXAFS signals were cut between 3 and 13 Å^{-1}. When a Fourier transform was applied, a Bessel window ($\tau = 3.5$) between 3 and 13 Å^{-1} was used for the $k^3\chi(k)$ form of the signal to determine the background of each spectrum.

(b) Data Analysis. The spectra were analyzed on an Indigo2 silicon graphics workstation using Xfine[43] for refinement and FEFF 6.01.[44−46] The goodness of fit parameter $R(k^3)$ quoted for refinement results was calculated as follows:

$$R(k^3) = \frac{\sum[k^3\chi(k)_{\mathrm{exp}} - \alpha k^3\chi(k)_{\mathrm{th}}]^2}{\sum(k^3\chi(k)_{\mathrm{exp}})^2} \times 100$$

where α is a normalization factor to modulate the FEFF S_0^2 (amplitude reduction factor) and $k^n\chi(k)_{\mathrm{exp}}$ and $k^n\chi(k)_{\mathrm{th}}$ are the experimental and the theoretical signals, respectively, with a value of $n = 3$ for the exponent of the wavevector k.

To compute X^2 (the statistical quantity chi-squared, not to be confused with $\chi(k)$, the EXAFS signal), the following definitions were used:

mean signal

$$\langle S\rangle = \sqrt{\frac{\sum_N \chi(k)^2_{\mathrm{exp}}}{N}}$$

mean background

$$\langle B\rangle = \sqrt{\frac{\sum_N (\chi(k)_{\mathrm{exp}} - \chi(k)_{\mathrm{FF}})^2}{N}}$$

with $\chi(k)_{\mathrm{FF}}$ being the Fourier-filtered signal and N the number of data points. The statistics X^2 was then computed as

$$X^2 = \frac{\sum_N (\chi(k)_{\mathrm{exp}} - \alpha\chi(k)_{\mathrm{th}})^2}{\langle B\rangle^2}$$

The quantity R_{B} (residual for background) is defined by the same formula as $R(k^3)$ (see above), with $\chi(k)_{\mathrm{th}}$ replaced by $\chi(k)_{\mathrm{FF}}$.

Spectra Simulation. We used the well-established FEFF 6.01 code[44−46] to generate ab initio X-ray absorption curves. The analysis started with a simulation of the MeCbl spectrum, using the coordinates of the crystal structure of methylcobalamin[47] and adjusting the amplitude reduction factor S_0^2, the energy shift ΔE, and the Debye−Waller factors σ_i^2 for each scattering path, allowing a maximum number of six scattering centers (NLEG) for any one scattering path and a maximum distance of 5.1 Å between a scattering center and the cobalt atom. Not surprisingly, in view of the large number of adjustable parameters, this led to good ($R(k^3) = 2.12\%$) agreement with the experimental $k^3\chi(k)$ curve.

Since the above criteria resulted in more than 500 paths involved in the calculation of the theoretical spectrum, we have simplified the model by omitting all contributions less than 10% of the largest contribution (first nitrogen shell of corrin ring). Only trivial differences are observed in $k^3\chi(k)$ as a result of this simplification (less than 1% in R), indicating that the omitted terms contributed mainly noise. Structurally, the model thus obtained was devoid of all the side-chain atoms, with the exception of the imidazole half of the dimethylbenzimidazole ring. This model (shown in Figure 3) was subsequently used for all calculations. We note that omitting the fused benzene ring plus the two methyl groups of the dimethylbenzimidazole base has practically no consequence on the calculated EXAFS spectrum, indicating that our EXAFS data would be unable to discriminate between the cobalt coordination of DMB and imidazole. The result of the above model simplification has another important ramification concerning multiple scattering: the contributions of multiple scattering paths (NLEG > 2) involving atoms from the equatorial corrin ring system together with atoms from one of the axial substituents were all below the 10% threshold, leading to the obvious consequence that this EXAFS analysis will be unable to determine the *orientation* of the axially coordinated imidazole ring. However, it also has the benefit that computations to determine the axial Co−N distance are considerably simplified, since contributions from the corrin ring can be left unchanged during a variation of the axial Co−N distance. More importantly, the individual σ_i^2 quantities obtained for the corrin moiety do not have to be physically meaningful, as they can be regarded as a mere footprint describing the scattering contribution of the corrin system.

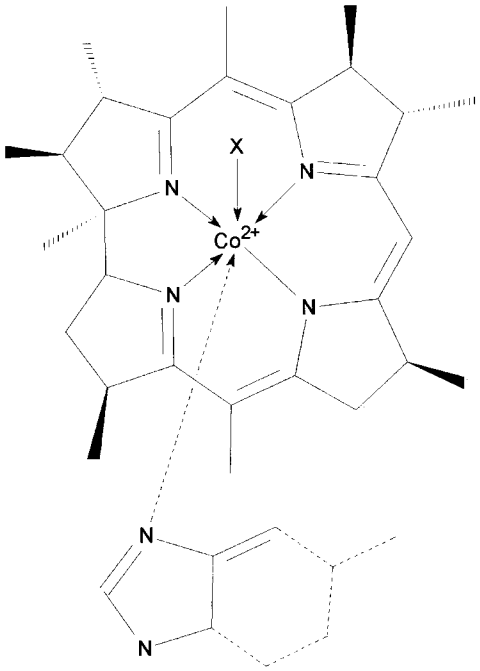

Figure 3. Structure of the model used for the simulation of the MeCbl spectrum, as well as for the interpretation of the protein spectra.

Eventually, the relative contributions to the EXAFS spectrum amounted to 3% for the methyl group (3 contributions), 16.3% for the axial ligand on the α side (DMB fragment, 22 contributions), and 80.6% for the equatorial corrin system (139 contributions), as given by the program FEFF. A control of these values was made by successively calculating spectra of models devoid of one of the axial ligands. Both these spectra gave a residual of about 3% with the theoretical spectrum calculated with the full model (i.e.. containing both axial ligands). Fourier transformation of the differences between spectra (calculated for the full model and those calculated for the model devoid of one axial ligand) showed that the contribution of the methyl group coincides with the equatorial Co−N distance, indicating that an independent determination of the Co−C distance will not be possible with the data available. The contribution (in Fourier space) of the atoms of the lower (α) ligand, on the other hand, consists of several peaks which only partially overlap with the contributions from equatorial atoms. Thus, we are confident that the data do indeed contain independent information on the distance to the α ligand.

(41) Lengeler, B.; Eisenberger, P. *Phys. Rev. B* **1980**, *21*.
(42) Eisenberger, P.; Lengeler, B. *Phys. Rev. B* **1980**, *22*, 3551−3562.
(43) Champloy, F.; Giorgi, M.; A., M.; Pierrot, M. *J. Synchrotron Res.* **1997**, *4*, 36−38.
(44) Rehr, J. J.; Alberts, R. C. *Phys. Rev. B.* **1990**, *41*, 8139−8416.
(45) Rehr, J. J.; Zabinsky, S. I.; Alberts, R. C. *Phys. Rev. Lett.* **1992**, *69*, 3397−3406.
(46) Rehr, J. J. *Jpn. Appl. Phys.* **1993**, *32*, 8−15.
(47) Rossi, M.; Summers, M. F.; Randaccio, L.; Toscano, P. J.; Glusker, J. P.; Marzilli, L. G. *J. Am. Chem. Soc.* **1985**, *107*, 1729−1738.

Table 1. Optimized EXAFS Parameters for Methylcobalamin with Positional Coordinates from the Crystal Structure[a]

	Fourier filtering		
	before	after	differences
S_0^2 (FEFF)	1.267	1.267	0
α	0.782	0.774	
$S_0^2 = \alpha S_0^2$ (FEFF)	0.994	0.980	0.014
$\langle\sigma^2_{Neq}\rangle$ (Å^2)	1.72×10^{-3}	1.84×10^{-3}	-0.12×10^{-3}
σ^2_{Nax} (Å^2)	7.82×10^{-3}	6.39×10^{-3}	-1.43×10^{-3}
σ^2_C (Å^2)	4.98×10^{-3}	4.77×10^{-3}	-0.21×10^{-3}
ΔE (eV)	−5.4	−6.0	0.6
$R(k^3)$	2.12	1.18	0.96
X^2	355		
N	313		
FT window (Å)	0.76−5.12		
$\langle S\rangle$	12.23×10^{-3}		
$\langle B\rangle$	2.232×10^{-3}		
$\langle S\rangle/\langle B\rangle$	5.48		
R_B (%)	1.42		

[a] The table lists parameters optimized with unfiltered and Fourier-filtered data, plus the respective differences. S_0^2 is the (dimensionless) amplitude reduction factor, which is obtained from the calculated value S_0^2(FEFF) after applying the normalization factor α (see text). $\langle\sigma^2_{Neq}\rangle$, σ^2_{Nax}, and σ^2_C are the Debye−Waller factors (in Å^2) from simple scattering (NLEG = 2) for the equatorial nitrogen (average value), the axial nitrogen and the axial carbon atoms, respectively. ΔE is the difference between the theoretical Fermi energy and the experimental value. $R(k^3)$, X^2, N, $\langle S\rangle$, $\langle B\rangle$, and R_B are as defined in Materials and Methods.

Table 2. Parameter Values from the Minimums of the Optimization[a]

	MeCbl	GLM	GLM−inh	MGM
$\langle S\rangle$	12.23×10^{-3}	15.64×10^{-3}	14.97×10^{-3}	17.18×10^{-3}
$\langle B\rangle$	2.232×10^{-3}	9.81×10^{-3}	3×10^{-3}	8.20×10^{-3}
$\langle S\rangle/\langle B\rangle$	5.48	1.59	5.00	2.09
R_B (%)	1.4	33.7	24.9	22.5
FT window	0.76−5.12	1.12−4.51	0.7−4.32	1.11−3.9
N	313	501	501	501
ΔE	−5.408	−5.81	−7.11	−6.31
Co−N_{ax}	2.18	2.17	2.19	2.15
rms[b]	0.09	0.1	0.08	0.1
X^2 [c]	292 (807)	92 (117)	595 (1065)	86 (88)
$R(k^3)$	2.1	35.9	26.2	31.5

[a] The quantities are as defined in Materials and Methods or in the legend to Table 1. [b] rms is the estimated root-mean-square deviation of the Co−N_{ax} bond length, obtained by fitting a Gaussian to the $R(k^3)$ curves of Figures 5 and 7, respectively. [c] The values in parentheses refer to the second minimum near 2.8 Å.

Relevant EXAFS parameters are listed in Table 1 for the optimization carried out with data before and after Fourier filtering. Simulated and experimental spectra for MeCbl are shown in Figure 4. Note that only the parameters obtained without Fourier filtering were used for the subsequent interpretation of protein spectra.

For a simulation of the protein spectra, the distance between histidine and cobalt was analyzed by generating 3D models of the atoms shown in Figure 3, using the crystal structure of methylcobalamin[47] as starting point. The generated structures differed only with respect to the axial coordination distance to the cobalt center, which was varied between 1.7 and 2.9 Å. The equatorial distances as well as the distance to the cobalt-coordinated methyl group were kept at the values observed in the MeCbl crystal structure.[47] For each of these models, the EXAFS spectrum was calculated using the parameter values for S_0^2, α, and the σ_i^2 extracted from the MeCbl spectrum. The value for ΔE was calculated for the minimum (see Table 2). All simulations were performed with unfiltered experimental spectra in order to prevent the introduction of artifacts by Fourier transform and back-transform. The results are presented in the form of optimization profiles, i.e., plots of the agreement factors $R(k^3)$ and X^2 versus the Co−N_{ax} distance, which are shown in Figure 5 for the protein samples. Experimental and simulated k^3-weighted EXAFS spectra are shown in Figure 6. As a control, we have also performed a self-test with the MeCbl data, the result of which is shown in Figure 7.

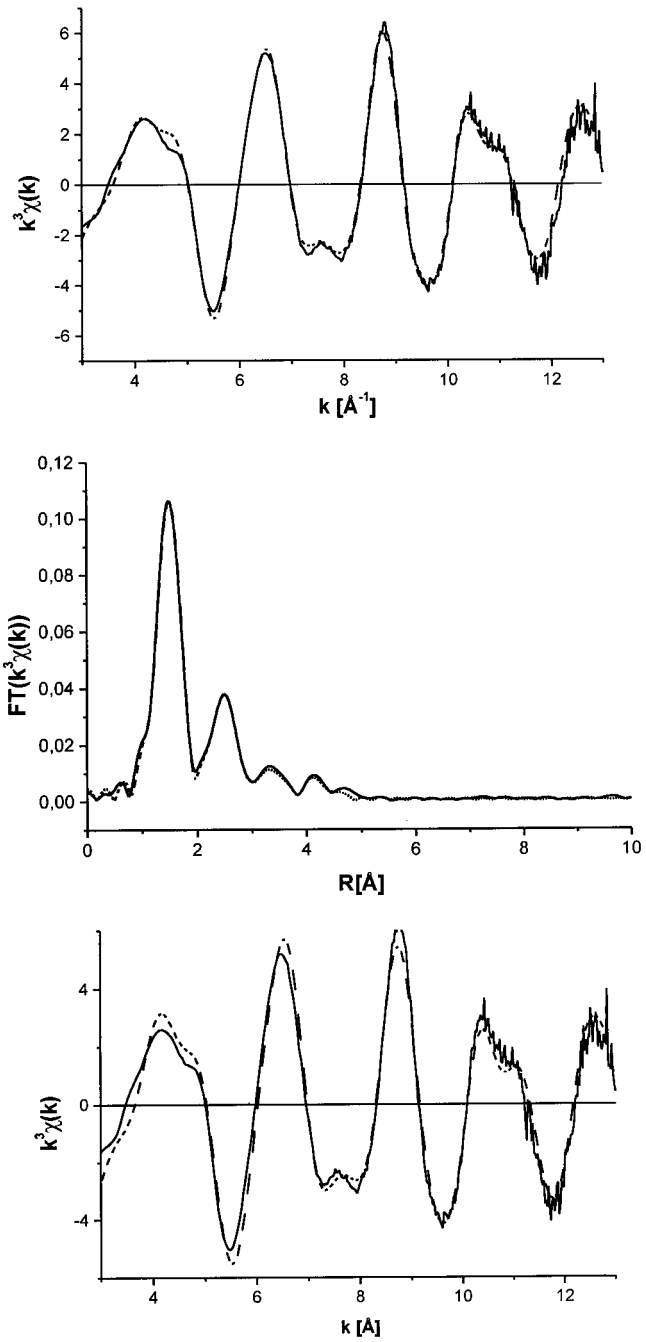

Figure 4. (a, top) Experimental (solid line) and simulated (dashed line) k^3-weighted EXAFS spectra for methylcobalamin before Fourier filtering. (b, middle) Fourier transforms of the spectra. (c, bottom) Experimental and simulated spectra for the minimum corresponding to a Co−N distance of 2.8 Å.

Results and Discussion

We have collected X-ray absorption data for the following samples: (1) crystalline MeCbl, as reference substance with a known 3D structure;[47] (2) recombinant glutamate mutase from *C. cochlearium*, reconstituted with MeCbl from components E and S overproduced in *E. coli* (GLM−MeCbl); (3) recombinant glutamate mutase, reconstituted with MeCbl in the presence of the inhibitor (2*S*,4*S*)-4-fluoroglutamate (GLM−MeCbl−Inh); (4) recombinant 2-methyleneglutaratemutase from *C. barkeri*, overproduced in *E. coli* and reconstituted with MeCbl (MGM−MeCbl).

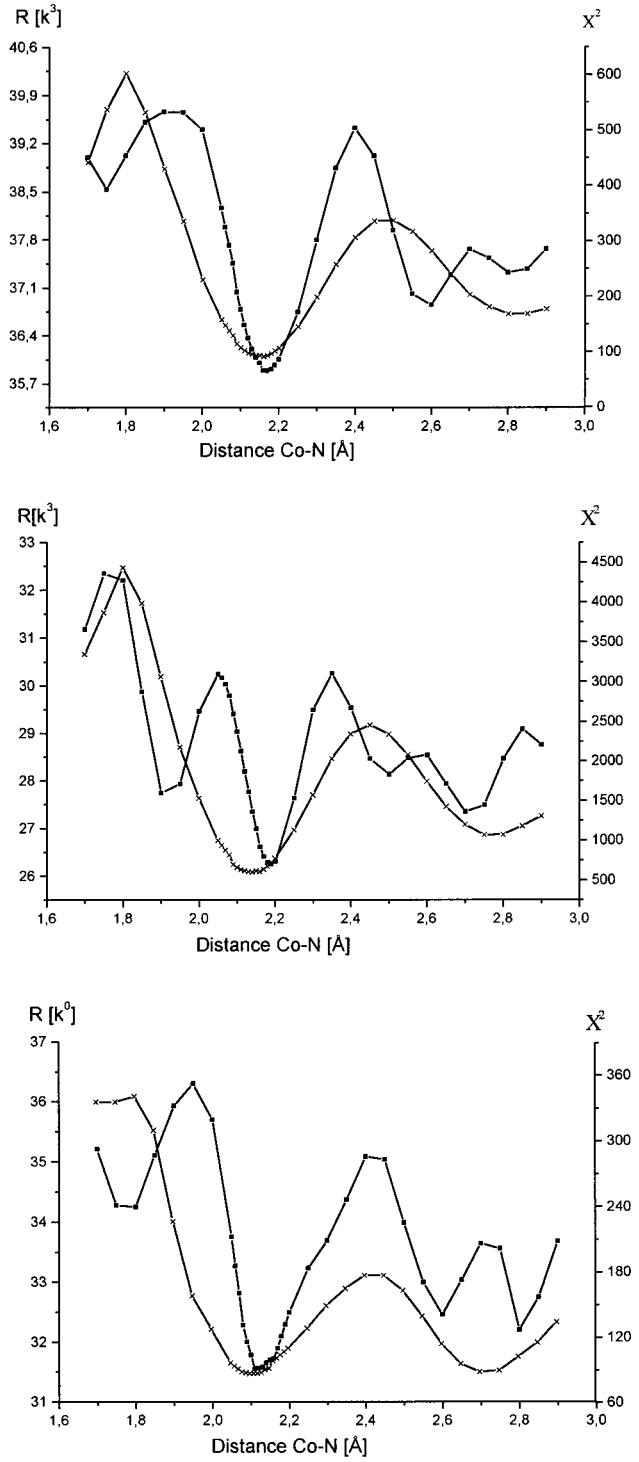

Figure 5. Optimization profiles ($R(k^3)$ factor (squares) and X^2 (crosses) versus the axial Co−N distance) for glutamate mutase (a, top), glutamate mutase with inhibitor (b, middle), and 2-methyleneglutarate mutase (c, bottom).

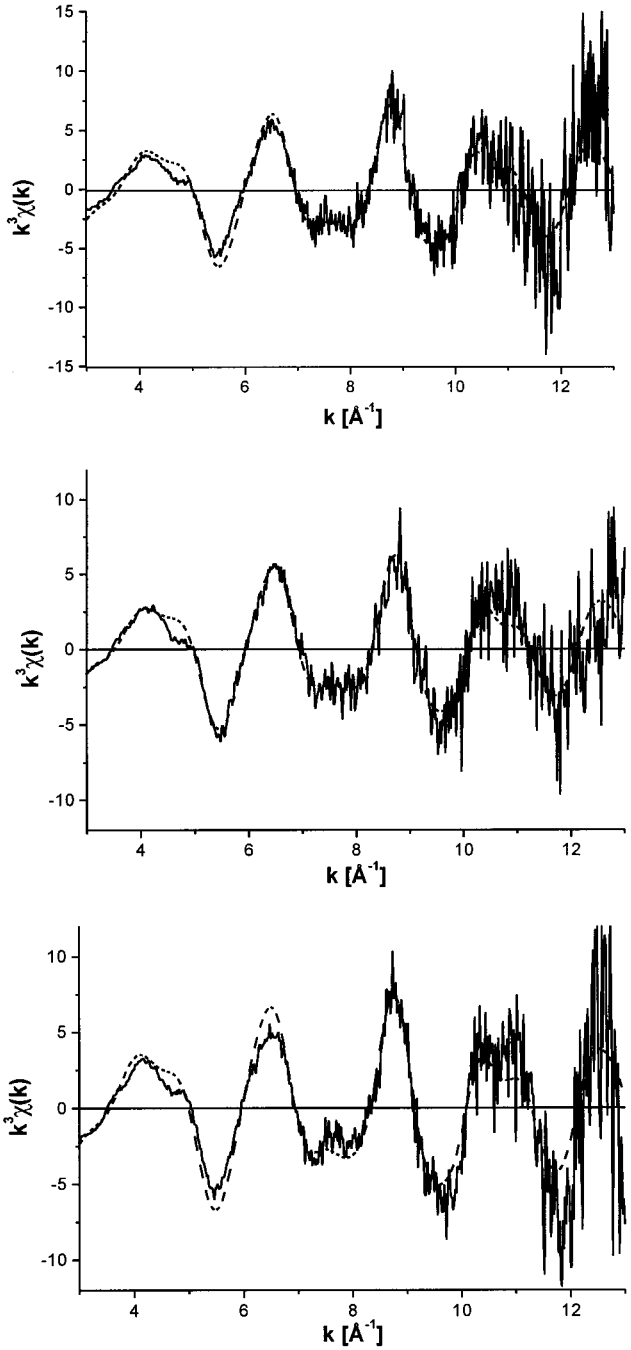

Figure 6. Experimental (solid line) and simulated (dashed line) k^3-weighted EXAFS spectra for glutamate mutase (a, top), glutamate mutase with inhibitor (b, middle), and 2-methyleneglutarate mutase (c, bottom).

XAS data were collected around the cobalt K-absorption edge at 20 K on freeze-dried and frozen protein, as described in Materials and Methods. The use of freeze-dried protein as opposed to protein in aqueous solution was necessary to obtain sufficient signal-to-noise ratio in view of the limited solubility of both proteins.

XANES Spectra. Figure 8 shows a superposition of the XANES part of the XAS spectra for the four samples. As a reference, spectra are also shown for aquocobalamin (aquoCbl,[13]) and for Cob(II)alamin (B_{12r}, K. Gruber and C. Kratky, unpublished data). Clearly, the four spectra originating from methyl-B_{12} species are more similar to one another than to the spectra of the reduced B_{12r} and the oxidized aquoCbl. All four methyl-B_{12} spectra show a pronounced preedge peak, indicating the presence of a covalently attached sixth carbon ligand to the cobalt center. This can be taken as strong evidence that the samples did indeed contain methyl-B_{12}, and it constitutes independent (from UV/visible, see Materials and Methods) proof for sample integrity during the XAS experiment.

Scrutiny of the XANES spectra reveals that, among the four spectra with MeCbl, the one of inhibited glutamate mutase (GLM−MeCbl−Inh) slightly deviates from the other three. However, since all spectra were taken on beam lines with an

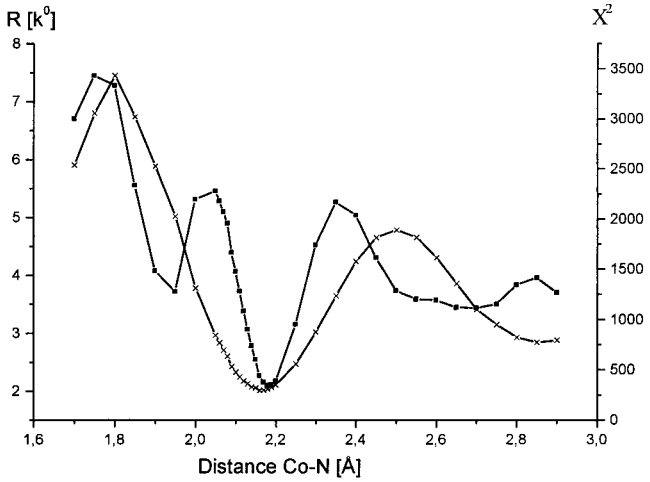

Figure 7. Optimization profile ($R(k^3)$ (squares) and X^2 (crosses) versus the axial Co−N distance) for the model compound methylcobalamin.

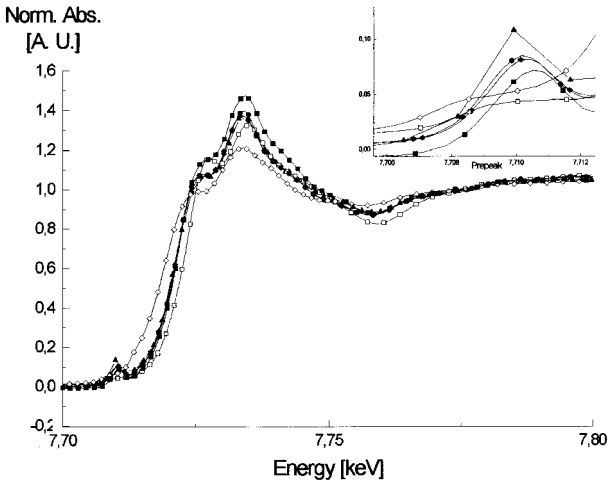

Figure 8. XANES part of the XAS spectra for methylcobalamin (full triangles), glutamate mutase without (full diamonds) and with (full squares) inhibitor, 2-methyleneglutarate mutase (full circles), aquocobalamin (open squares), and cob(II)alamin (open diamonds).

inherent resolution around 2 eV, attempts toward a quantitative analysis of the XANES spectra[16] are not warranted in this case.

Simulation of the EXAFS Spectra. The result of the spectra simulations are presented in the form of optimization profiles, i.e., as plots of the agreement factors $R(k^3)$ and X^2 as a function of the distance between the cobalt center and axial nitrogen ligand. Note that we have kept all other distances, i.e., the distance from cobalt to the equatorial corrin nitrogen atoms and to the methyl carbon atom, at the value observed in the crystal structure of methylcobalamin.[47] While, as outlined above, not all atoms of the methylcobalamin system were used for computing theoretical spectra, those that were used had the same arrangement (with the exception of an axial movement of the base) as in the MeCbl crystal structure.

Figure 7 shows the optimization profile for the reference compound methylcobalamin. Not surprisingly, the plot of $R(k^3)$ versus the Co−N_{ax} distance shows the deepest minimum around 2.18(9) Å ($R(k^3) = 2.12\%$). This distance agrees (within the respective accuracy of the two methods) with the value observed in the crystal structure of MeCbl (2.19 Å). There are two other minimums for $R(k^3)$ within the range of simulated Co−N_{ax} distances: a relatively sharp one near 1.9 Å—which coincides with the mean distance between cobalt and the four equatorial corrin nitrogen atoms—and a broad one between 2.5 and 2.8 Å. While the minimum near 1.9 Å does not coincide with a minimum of X^2, the one at longer Co−N_{ax} distances does. However, the fit between experimental and simulated $k^3\chi(k)$ signal is marginally better for the correct minimum (Figure 4a) than for the spurious one (Figure 4c).

The corresponding optimization profiles for the three protein samples (MeCbl−reconstituted GLM without and with inhibitor and MeCbl−reconstituted MGM) are shown in Figure 5. All three profiles are quite similar to the one of pure MeCbl (Figure 7), compatible with a similar Co−N_{ax} distance between the three protein samples and the MeCbl sample. However, due to the lower data quality compared to the MeCbl sample, the minimum corresponding to a Co−N_{ax} distance between 2.6 and 2.8 Å cannot strictly be excluded on the basis of the EXAFS evidence alone.

Thus, our EXAFS evidence is most compatible with a "normal" Co−N bond in the two coenzyme B_{12}-dependent enzymes glutamate mutase and 2-methyleneglutarate mutase, in contrast to the EXAFS results on MCM[16] and to the X-ray evidence on MCM,[11] GLM,[12] and diol dehydratase.[18] While a detailed appraisal of the crystallographic results is beyond the scope of the present paper , we note that crystallography of B_{12} proteins has repeatedly been troubled by the problem of locating electron density for the "upper" cofactor ligand.[10−12] We have recently obtained evidence in our laboratory that these problems are at least partly due to X-ray-induced reduction of the cofactor.

Both enzymes of the present study (GLM and MGM) were reconstituted with methylcobalamin, since they are unstable and prone to Co−C bond homolysis when reconstituted with AdoCbl. Reconstitution with MeCbl was therefore chosen as a remedy against partial homolysis, which has hampered the analysis of the MCM crystal structure.[11] It has been observed that addition of the inhibitor (2*S*,4*S*)-4-fluoroglutamate to active glutamate mutase (reconstituted with AdoCbl) leads to Co−C bond homolysis.[28] If inhibitor (or substrate) binding caused bond homolysis via stretching of the axial Co−N bond, we would expect to observe at least some bond elongation also in the inactive enzyme reconstituted with MeCbl (which is less likely to homolyze due to the instability of the formed methyl radical). Interestingly, addition of the inhibitor to glutamate mutase led to no detectable change in the axial Co−N bond length, although (as shown by the ITC experiment) the inhibitor binds strongly to the inactive enzyme with the expected stoichiometry.

Previous Evidence for a Long Axial Co−N Bond in a Coenzyme B_{12}-Dependent Enzyme. First evidence for an "abnormally" long axial Co−N bond came from the crystal structure (at 2 Å nominal resolution) of methylmalonyl-CoA mutase from *Propionibacterium shermanii* in complex with coenzyme B_{12} and with the partial substrate desulfo-CoA.[11] Here, a 2.53 Å long bond was observed between the cobalt center and Nϵ1 of the coordinating imidazole of His-A610. In addition, the cobalt atom was found to be displaced by 0.11 Å toward the coordinating imidazole. While this long bond (exceeding the corresponding bond lengths observed in cobalamin crystal structures by at least 0.3 Å) was linked to a possible mechanism for enzyme-assisted homolysis of the trans-annular cobalt−carbon bond, the significance of the observation suffered from the lack of observability of the "upper" cobalt ligand. Thus, it was concluded from aposteriori evidence that a mixture of cofactors in Co(III) and Co(II) states had been present in the crystal, with the Co(II) form predominating. In line with this interpretation is also the observed displacement of the cobalt atom from the corrin ring plane toward the imidazole Nϵ1. In fact, a very similar (0.12 Å) displacement of the cobalt center

toward the axial ligand was observed in the crystal structure of cob(II)alamin.[7] The crystal structures of Glm−CNCbl and Glm−MeCbl also showed a significant elongation of the axial Co−N bond,[12] but again, the significance of this observation is compromised by disorder due to the occurrence of the cofactor in a mixture of oxidation states.

Recently, the result of EXAFS experiments on MCM with adenosyl-B_{12} and aquo-B_{12} cofactors was reported.[16] Despite methodological differences to the present work with respect to data processing and spectra simulation (different resolution, use of Fourier-filtered versus unfiltered data, different use of the model complex, etc.) the dependence of the residual versus the axial Co−N_{ax} distance has a shape qualitatively similar to the curves (see Figure 5) obtained with our protein samples: in both cases, three minimums are typically observed in the $R(k^3)$ curves, near 1.9 and 2.2 and beyond 2.5 Å. While for MCM, the EXAFS data alone did not permit an unequivocal decision between a shorter (∼2.2 Å) and a longer (∼2.5 Å) Co−N_{ax} distance, the longer distance was preferred in view of the crystallographic data of the mutase complex.[11] In fact, there appears to be somewhat conflicting evidence on this issue, since optical spectroscopy (very close similarity in the 525 nm absorption maximum of free and enzyme-bound AdoCbl) gives no indication for a significant change in the metal coordination upon cofactor binding to the apoenzyme (base off AdoCbl has an absorption maximum near 460 nm,[48] and one might expect a blue-shift of the 525 nm absorption maximum upon weakening of the Co−imidazole bond).[16] While the interpretation of EPR evidence on the reduced (Co(II)) B_{12} cofactor bound to MCM,[49,50] GLM,[51] and MGM[52] is often complicated by the appearance of several paramagnetic species, the hyperfine coupling constant in the spectrum of MCM with a reduced cofactor is indistinguishable from the one of free Cob(II)alamin in solution. Thus, also the EPR data of the Co^{II}MCM species do not provide evidence for a weaker interaction.[16]

Expectations from Coordination Chemistry. From single-crystal X-ray diffraction results on cobalamins, values for the axial Co−N distance around 2.2 Å have been observed in the more accurate crystal structures of cobalamins with an organo substituent in the β ("upper") position.[53−55] However, the dimethylbenzimidazole base is replaced by a protein-derived imidazole in MCM,[11,50] GLM,[12,27] and MGM (G. Broeker, F. Kroll, and W. Buckel, unpublished result). Crystallographic evidence and chemical plausibility predict a shortening of the Co−N bond when DMB is replaced by the less bulky and more nucleophilic imidazole, in view of the higher pK_a of imidazole (7.0[56]) as compared to dimethylbenzimidazole (6.0[57]) and

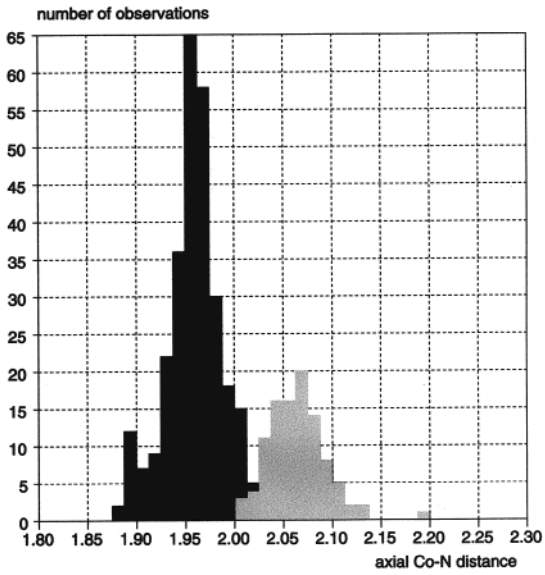

Figure 9. Histogram of axial Co−N distances in octahedral cobalt(III) complexes with at least five nitrogen ligands. The gray bars denote compounds with carbon as the sixth ligand; the black ones originate from compounds with nitrogen or oxygen as the sixth ligand.

α-ribazole (5.6[58]). Accordingly, the crystal structure of Co−β-cyanoimidazolylcobamide,[59] i.e., the vitamin B_{12} analogue with the cobalt-coordinating DMB replaced by imidazole, shows a 0.04 Å shorter axial Co−N bond than cyanocobalamin (1.97 versus 2.01).

In view of the small number of published high-resolution cobalamin crystal structures,[54,60] it is worthwhile to consider the coordinative preferences of cobalt centers in a less restricted sample. We have searched the Cambridge Structural Data Base[61,62] for crystal structures containing a cobalt atom in oxidation state III, surrounded by four equatorial nitrogen atoms in approximate square-planar arrangement (as specified by the six N−Co−N bond angles) and at least one axial nitrogen atom. The (bimodal) disribution of 374 axial Co−N bond lengths with C, N, or O as trans-axial ligand is shown in Figure 9). Detailed analysis reveals that the maximum between 1.87 and 2.03 Å originates from structures with N or O as trans-axial ligand, whereas the maximum at longer Co−N distance (beyond 2.03 Å) originates from structures with carbon as the trans-axial ligand. While B_{12} structures have been excluded from this analysis, the one outstanding structure with a Co−N distance around 2.19 Å corresponds to a highly strained B_{12} model compound (*trans*-bis(dimethylglyoximato)isopropyl(2-aminopyridine)−cobalt(III), entry CAPJEI[63]). An axial Co(III)−N distance of 2.53 Å is thus unprecedented and would imply a considerably strained metal coordination, even considering that the known alkylcobalamins cluster on the far right of the distribution, with axial Co−N distances around 2.2 Å.[53−55]

(48) Gianotti, C. In *Electronic spectra of B_{12} and related systems*; Dolphin, D., Ed.; Wiley and Sons: New York, 1982; pp 393−340.
(49) Padmakumar, R.; Banerjee, R. *J. Biol. Chem.* **1995**, *270*, 9295−9300.
(50) Padmakumar, R.; Taoka, S.; Padmakumar, R.; Banerjee, R. *J. Am. Chem. Soc.* **1995**, *117*, 7033−7034.
(51) Leutbecher, U.; Albracht, S. P. J.; Buckel, W. *FEBS Lett.* **1992**, *307*, 144−146.
(52) Michel, C.; Albracht, S. P. J.; Buckel, W. *Eur J Biochem* **1992**, *205*, 767−773.
(53) Kratky, C.; Kräutler, B. In *Chemistry and Biochemistry of B_{12}*; Banerjee, R., Ed.; John Wiley and Sons: New York, 1999; pp 9−41.
(54) Gruber, K.; Jogl, G.; Klintschar, G.; Kratky, C. In *High-resolution crystal structures of cobalamins*; Kräutler, B., Arigoni, D., Golding, B. T., Eds.; Wiley-VCH: Weinheim, 1998; pp 335−347.
(55) Glusker, J. P. In *B_{12}*; Dolphin, D., Ed.; Wiley-Interscience: New York, 1982; Vol. 1, pp 23−107.
(56) Datta, S. P.; Grzybowski, A. K. *J. Chem. Soc. B* **1966**, 136−140.
(57) Davies, M. T.; Mamalis, P.; Petrow, V.; Sturgeon, B. *J. Pharm. Pharmacol.* **1951**, *3*, 420−430.
(58) Brown, K. L.; Hakimi, J. M. *J. Am. Chem. Soc.* **1986**, *108*, 496−503.
(59) Kräutler, B.; Konrat, R.; Stupperich, E.; Färber, G.; Gruber, K.; Kratky, C. *Inorg. Chem.* **1994**, *33*, 4128−4139.
(60) Rossi, M.; Glusker, J. P. In *Molecular structure and dynamics*; Liebmann, J. F., Greenberg, A., Eds.; VCH: New York, 1988; Vol. 10, pp 1−58.
(61) Allen, F. H.; Bellard, S.; Brice, M. D.; Cartwright, B. A.; Doubleday, A.; Higgs, H.; Hummelink-Peters, T.; Kennard, O.; Motherwell, W. D. S.; Rodgers, J. R.; Watson, D. G. *Acta Crystallogr.* **1979**, *B35*, 2331−2339.
(62) Allen, F. H.; Kennard, O.; Taylor, R. *Acc. Chem. Res.* **1983**, *16*, 146−153.
(63) Summers, M. F.; Toscano, P. J.; Bresciani-Pahor, N.; Nardin, G.; Randaccio, L.; Marzilli, L. G. *J. Am. Chem. Soc.* **1983**, *105*, 6259−6263.

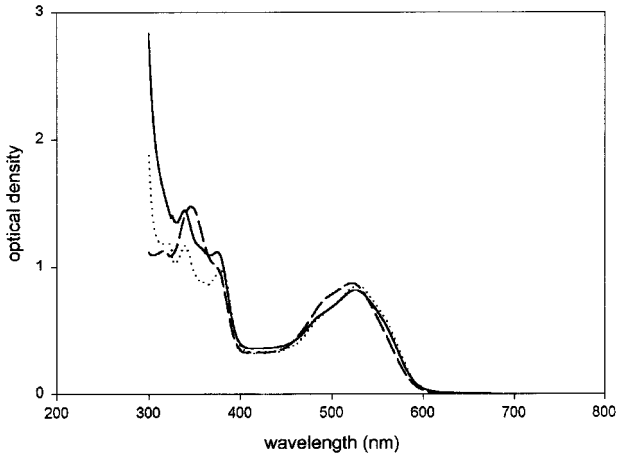

Figure 10. UV/visible spectra of free methyl cobalamin (dashed curve), of MeCbl reconstituted glutamate mutase (full line), and of a redissolved MeCbl−GLM sample after the EXAFS experiment (dotted line).

We note that the situation is somewhat different for cobalt(II). Here, axial Co(II)−N distances up to 2.265 Å ((*R*)-phenetylaminotetraphenylporphyrin−cobalt(II), entry HAMBAY,[64]) were so far observed in pentacoordinated complexes and up to 2.436 Å in symmetrically hexacoordinated Co(II) complexes (bis(piperidine)-α,*β*,*γ*,*δ*-tetraphenylporphinato−cobalt(II), entry PTPORC).[65] The occurrence of longer axial distances in the case of the reduced cobalt(II) is also accompanied by a larger *spread* of observed axial distances as a function of different chemical environments as compared to cobalt(III).

Both EXAFS experiments (the one on MCM[16] and the one reported in the present paper) clearly dealt with alkyl-substituted cobalt(III), for which an unstrained axial cobalt−nitrogen distance below 2.2 Å is predicted from isolated cofactor data. If the elongation to 2.53 Å in MCM were entirely the result of protein-mediated steric effects, it would be of interest to estimate the required amount of strain energy. Co−C force constants have recently been determined for alkylcobalamins,[66] but the corresponding Co−N force constants for the trans-annular bond can only be estimated from IR spectroscopic data for model complexes.[67] From these data, it is reasonable to estimate a value of 250 cm^{-1} for the ν(Co−N) stretching frequency, which would lead to about 14 kJ/mol strain energy for an elongation of this bond by 0.33 Å from its equilibrium value, assuming a harmonic potential.

Relevance for the Mechanism of Co−C Bond Cleavage. Notwithstanding the validity of the experimental observation of a long Co−N_{ax} bond in B_{12} proteins, it is worth considering whether such a protein-induced stretching of the trans-annular bond would contribute significantly to the homolysis of the Co−C bond as suggested.[11,15] A protein-mediated deformation of the B_{12} moiety can only be catalytically effective if the deformed geometry more closely resembles the Co(II) reaction product than the undeformed adenosyl-B_{12} species. However, the crystal structure of Cob(II)alamin[7] revealed a very similar molecular geometry of the B_{12} part to adenosylcobalamin.[14] With regard to the Co−N_{ax} bond, it was shown that this bond is even shorter in the (5-coordinated) Co(II) species (2.16 versus 2.21 Å), but as a result of a "downward" displacement of the cobalt atom toward the α-coordinated DMB ligand, the distance between DMB and corrin ring is more or less the same. Evidently, the inherently larger covalent radius of cobalt(II) as opposed to Co(III) is more that offset by the strongly donating trans ligand in alkylcobalamins. As a result of these observations, preferential binding of the two separated homolysis fragments was suggested as a mechanism for protein-mediated Co−C bond homolysis.[7] For methylmalonyl CoA mutase, such a mechanism has recently been suggested based on crystallographic data from substrate-free MCM.[8]

Acknowledgment. This research was supported by the Österreichischer Fonds zur Förderung der wissenschaftlicher Forschung FWF (Project 11599), by the European Commission (TMR project ERB 4061 PL 95-0307), and by the Deutsche Forschungsgemeinschaft. Synchrotron XAS data were collected at the EMBL-EXAFS beamline D2 at the DESY in Hamburg, Germany, and at LURE-DCI EXAFS III station in Orsay, France. We thank Walter Keller for his help with the ITC experiment, Oliver Sauer, Andrea Schmidt, and Kim Scheuring for help during EXAFS data collection, and Karl Gruber for stimulating discussions.

JA990349Q

(64) Byrn, M. P.; Curtis, C. J.; Hsiou, Y.; Khan, S. I.; Sawin, P. A.; Tendick, S. K.; Terzis, A.; Strouse, C. E. *J. Am. Chem. Soc.* **1993**, *115*, 9480−9497.

(65) Scheidt, W. R. *J. Am. Chem. Soc.* **1974**, *96*, 84.

(66) Dong, S. L.; Padmakumar, R.; Banerjee, R.; Spiro, T. G. *Inorg. Chim. Acta* **1998**, *270*, 392−398.

(67) Alexander, V. *Inorg. Chim. Acta* **1993**, *204*, 109−124.